

Characterization of photodiodes as transfer detector standards in the 120 nm to 600 nm spectral range

*P. Kuschnerus, H. Rabus, M. Richter,
F. Scholze, L. Werner and G. Ulm*

Abstract. Using spectrally dispersed synchrotron radiation of continuously tuneable wavelength as delivered by the ultraviolet (UV) and vacuum ultraviolet (VUV) calibration facility of the Physikalisch-Technische Bundesanstalt (PTB) at the electron storage ring BESSY I in Berlin, various types of silicon photodiode have been examined for their radiometric performance in the 120 nm to 600 nm spectral range. Their absolute spectral responsivity was determined with a typical relative uncertainty of 0.7 % using the synchrotron-radiation cryogenic electrical-substitution radiometer, SYRES, as primary detector standard. Particular emphasis has been given to the study of radiation-damage effects at wavelengths below 250 nm. In addition, the reflectance of the photodiodes was measured to determine their internal quantum efficiency. Using a physical model for the internal losses, the mean energy to create an electron-hole pair in silicon was derived.

1. Introduction

Silicon photodiodes are widely appreciated as easy-to-operate and low-cost photon detectors for various spectral ranges, from the infrared to x-rays. In the visible and adjacent near-infrared and near-ultraviolet spectral ranges, silicon photodiodes are used for the realization and dissemination of the spectral-responsivity scale [1-3]. The silicon pn-junction diodes employed have proved to be spatially uniform [4], highly linear [5] and stable [6] in the wavelength range 250 nm to 1000 nm. For prolonged exposure to UV or VUV radiation at wavelengths below 250 nm, however, a strong degradation of their spectral responsivity is observed [7, 8]. This radiation-induced ageing effect is generally attributed to the formation of traps of charge carriers in the region of the oxide passivation layer or the oxide/silicon interface. The resulting electric field influences charge separation within the depletion zone [9]. For pn-junction photodiodes this leads to a reduction in responsivity. As a consequence, np-type photodiodes have been developed that, unlike pn devices, have proved to be stable under prolonged exposure to soft x-ray radiation [10]. For Schottky-barrier photodiodes, oxide trap formation is impossible due to the absence of an oxide layer so that radiation damage originating via this mechanism is not expected [11].

The purpose of this study is to compare the following types of silicon photodiode for their suitability as transfer detector standards in the 120 nm to 600 nm spectral range:

- (a) diffusion type pn-junction diodes (Hamamatsu types S1337 and S5226),
- (b) diffusion type np-junction diodes with nitrided-oxide passivation layer for increased radiation hardness (International Radiation Detectors types AXUV-100G and UVG-100),
- (c) a new type of Schottky-barrier silicon photodiode with a PtSi front contact (PtSi-n-Si) developed at the Swiss Federal Institute of Technology [8].

Particular emphasis was given to the study of ageing effects in their response under prolonged exposure. In the spectral range of their stability the absolute spectral responsivity and the reflectance of the photodiodes were determined to derive their internal quantum efficiency.

The experiments were performed at the laboratory for UV and VUV radiometry of the Physikalisch-Technische Bundesanstalt. A detailed description of the detector-calibration facility for the UV and VUV spectral ranges at the electron storage ring BESSY I in Berlin has been given elsewhere [12]. For the investigations of this study in the spectral range between 120 nm and 600 nm, the 1 m/15° McPherson-type normal-incidence monochromator was operated with the Al/MgF₂-coated grating in combination with the Al-coated condenser mirror, employing the appropriate order-sorting filters (Figure 10 in [12]). In the 120 nm to 170 nm spectral range, the photo-emission current

P. Kuschnerus, H. Rabus, M. Richter, F. Scholze, L. Werner and G. Ulm: Physikalisch-Technische Bundesanstalt, Abbestrasse 2-12, D-10587 Berlin, Germany.

of the refocusing mirror was used to monitor temporal variations of the radiant power; for wavelengths longer than 170 nm, the fused-silica beam-splitter monitor was used.

2. Spectral responsivity

The spectral responsivity of the photodiodes was measured absolutely using the synchrotron-radiation cryogenic electrical-substitution radiometer, SYRES, as primary detector standard [12]. For the experiments a pivoting platform was installed at the rear end of the beamline. The platform bearing the SYRES and a detector station to house the diodes was used to locate the different detectors alternately in the beam path. The spectral responsivity of the photodiodes was obtained as the ratio of the diode photocurrent to the radiant power measured by the SYRES.

Figure 1 shows the results for four different types of photodiode. The upper part shows the spectral responsivity of the S5226 Si pn (circles) and the AXUV-100G Si np (triangles) photodiodes. The open circles correspond to measurements performed at wavelengths where the S5226 photodiodes degrade in their spectral

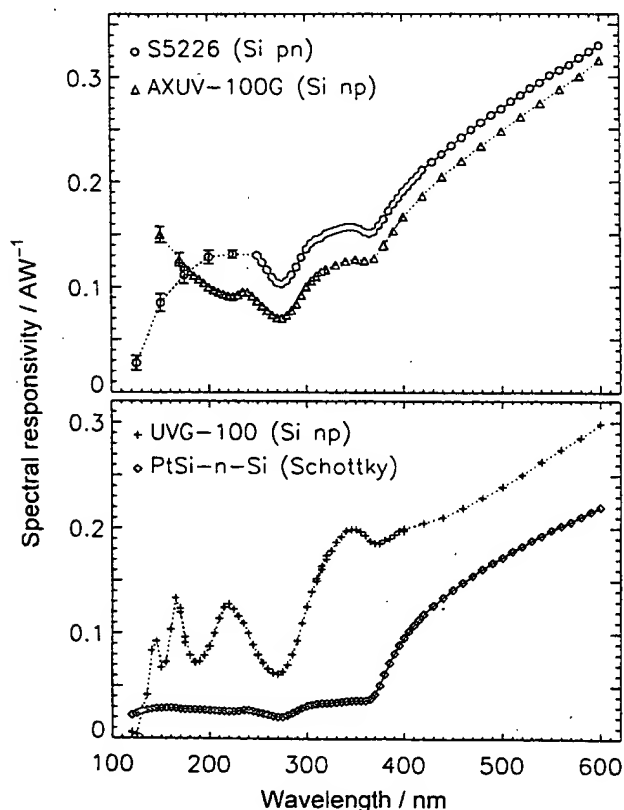


Figure 1. Spectral responsivity of several types of silicon photodiode in the 120 nm to 600 nm spectral range. The open circles represent data points for the pristine spectral responsivity at wavelengths where the S5226 is prone to rapid radiation damage as indicated by the enlarged error bars. For all other data points the standard relative uncertainty of the spectral responsivity is about 0.7 %.

responsivity when irradiated. In this case the data points mark the initial spectral responsivity of pristine samples.

The lower part of Figure 1 displays the spectral responsivity of the UVG-100 Si np photodiode and the new PtSi-n-Si Schottky-type photodiode in comparison. In addition to the features around 280 nm and 360 nm that are due to absorption maxima of silicon, the UVG-100 shows further structures at shorter wavelengths that are caused by interference effects in the comparatively thick oxide passivation layer (about 160 nm thick compared with about 27 nm for the S5226). The results for the second type of p-on-n photodiode, the Hamamatsu S1337, have been omitted in Figure 1 as they almost coincide with the results of the S5226 photodiode.

In general, the typical relative uncertainty of the spectral responsivity data shown in Figure 1 is about 0.7 % in the 170 nm to 600 nm spectral range [12], and about 1 % in the 120 nm to 170 nm spectral range. This does not, of course, apply to wavelengths where the diodes are prone to radiation damage, for which the larger uncertainties are indicated by the error bars in Figure 1.

3. Radiation damage

To investigate their UV stability, the photodiodes under study were subjected to prolonged exposure to narrow-bandwidth radiation of fixed wavelengths. Typical values of the radiant power in the incident beam were of the order of 10 μ W, the beam size was about 2 mm by 1 mm (FWHM), and exposure times amounted to about 30 minutes or more. The diode response was measured as a function of time. Combination with the simultaneously recorded beam-monitor signal allowed the relative variation of the spectral responsivity over the course of the experiment to be derived. From the known irradiance profile [12] and the absolute value of the initial spectral responsivity of the particular photodiode, the exposure time was converted to radiant exposure. Sample results are displayed in Figure 2.

Figure 2a shows the change of the relative spectral responsivity of pn-junction photodiodes (Hamamatsu, S5226) as a function of the radiant exposure for irradiation at three different wavelengths. At 250 nm the spectral responsivity of the diode remains constant, whereas at shorter wavelengths a rapid degradation is observed, the rate of radiation damage increasing with decreasing wavelength. At 150 nm the radiation-damage effect is already significant, while at 125 nm, the spectral responsivity is seen to converge to a reduced value of less than 25 % of the initial value. It should be noted that the solid lines in Figure 2 are fitted curves that were derived from the assumption that the radiation damage shows a spatial variation, the local degradation being proportional to the respective irradiance value. The excellent reproduction of the functional dependence $s(H)$ is regarded as an additional proof that the radiant

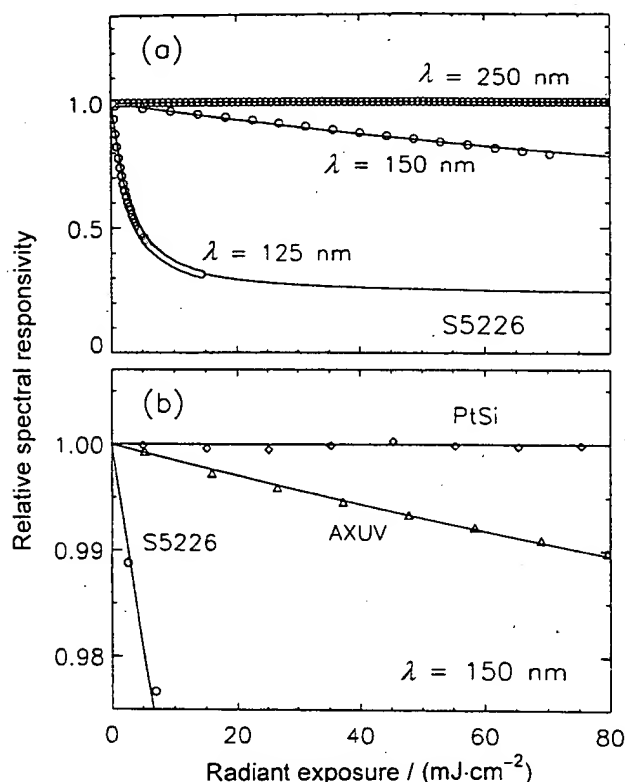


Figure 2. Relative spectral responsivity as a function of the radiant exposure: (a) for a Hamamatsu S5226 pn-junction photodiode for irradiation at wavelengths of 250 nm, 150 nm, and 125 nm; (b) for an S5226, an IRD AXUV-100G np-junction diode and a PtSi-n-Si Schottky-barrier diode (ETH Zürich) for irradiation at 150 nm.

exposure H is the decisive experimental parameter determining the magnitude of the degradation [12].

Figure 2b shows the corresponding results for irradiation at a wavelength of 150 nm of an np-junction photodiode (IRD, AXUV-100G) with a nitrided-oxide passivation layer and a PtSi-n-Si Schottky-barrier photodiode (ETH Zürich, PtSi). While the radiation-damage effect of the AXUV-100G photodiode is less pronounced than in the case of the pn-junction diodes, the PtSi photodiode shows no change in spectral responsivity.

For a convenient comparison of the UV stability of the different diode types, the initial gradient α of the relative spectral responsivity versus radiant exposure curve

$$\alpha = \frac{1}{s_0} \frac{ds}{dH} \quad (1)$$

is used as a measure of merit. Figure 3 shows the initial gradient values obtained for the different photodiode types as a function of wavelength in the 120 nm to 300 nm spectral range. For the PtSi-n-Si photodiodes, the initial gradient was found to be below the lower detection limit of $5 \times 10^{-3} \text{ cm}^2 \cdot \text{J}^{-1}$ for all wavelengths investigated. All the other types of photodiode examined show slope values in excess

of $0.02 \text{ cm}^2 \cdot \text{J}^{-1}$ for wavelengths less than 250 nm. At wavelengths below the onset of absorption in the SiO₂ passivation layer at about 150 nm, the initial degradation rate of the pn-junction photodiodes increases dramatically with decreasing wavelength to values up to about $300 \text{ cm}^2 \cdot \text{J}^{-1}$ at 125 nm. For the AXUV-100G photodiodes, an initial degradation rate exceeding the detection limit is encountered for wavelengths between 125 nm and 225 nm. The second type of np-junction photodiode, the UVG-100, which is passivated with a nitrided-oxide layer 160 nm thick rather than 5 nm as in the case of the AXUV-100G diodes, shows significant changes only for wavelengths between 175 nm and 225 nm. It should be noted that both inversion-type photodiodes show no change in their spectral responsivity when irradiated at 125 nm wavelength, which is in close proximity to the Lyman- α line that is customarily used for stability tests in the VUV [10].

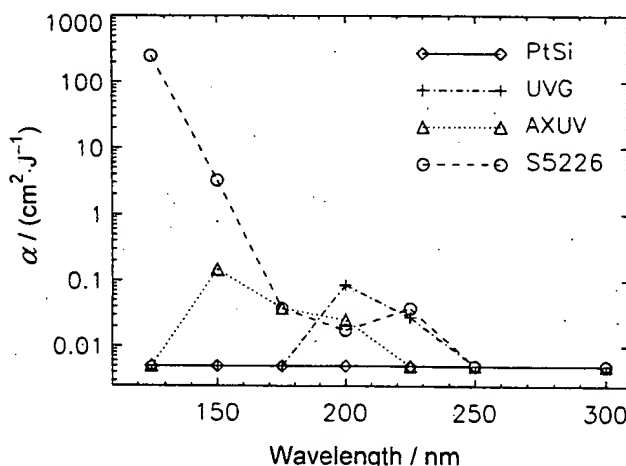


Figure 3. Initial gradient α of the change of the relative spectral responsivity with increasing radiant exposure as a function of the wavelength for various photodiodes. The value $5 \times 10^{-3} \text{ cm}^2 \cdot \text{J}^{-1}$ is the lower detection limit.

4. Spatial uniformity

Tests of the spatial uniformity of the spectral responsivity across the sensitive surface of the diodes have been performed at various wavelengths. The diodes were scanned behind a pinhole of 0.25 mm diameter, used to confine the synchrotron-radiation beam size. Due to the nonuniform beam profile, the use of the pinhole introduced a strong sensitivity to minor changes in the beam position; these can be ignored when performing calibration measurements using the full beam. Thus, the lower detection limit for relative variations of the spectral responsivity was comparatively large, about 0.8 % [8]. In order to verify the results, additional measurements have therefore been performed using intensity-stabilized laser radiation at 257.3 nm wavelength of a frequency-doubled argon ion laser [13]. The laser output is stable to few parts

in 10^5 [14]. For the uniformity measurements, the laser beam was focused to a circular Gaussian spot of 0.25 mm diameter, and the photodiodes were scanned in two dimensions across the beam. For the summary of results given in Table 1, the relative standard deviation of the spectral responsivity was calculated, taking into account only data points located within a circular area of 6 mm diameter in the centre of the sensitive surface. The second row in Table 1 gives the contribution to the relative uncertainty resulting from calibration of the photodiode at the UV-VUV detector calibration facility, using the full beam which is aligned with the centre of the photodiode active area to within ± 0.5 mm in both directions.

5. Reflectance and internal quantum efficiency

In order to study the reflectance of the diodes for different angles of incidence, a reflectometer [15] was installed at the end of the UV-VUV detector calibration facility such that the samples under investigation were located at the beam-line focal point. The angle of incidence to the diodes was varied from 4° to 70° , and the reflected radiant power and the signal of the diode under study were recorded in parallel. The radiant power of the specularly reflected beam was measured using a calibrated photodiode. The angle of incidence to the reflectance-detection diode was slightly off-normal to avoid retroreflection to the diode under study.

To avoid radiation damage, the reflectance measurements on the diffusion-type photodiodes were, in general, restricted to wavelength ranges in which the spectral responsivity of the respective type of diode proved to be stable under irradiation or showed only negligible changes. This applies to the 200 nm to 600 nm wavelength range in the case of the np-junction photodiodes, and to the 250 nm to 600 nm spectral range in the case of the pn-junction diodes. As an example, Figure 4a shows the measured reflectance curves of an AXUV-100G and an S1337 photodiode for 4° off-normal incidence of the radiation. The typical standard relative uncertainty of the measurement amounts to 1.5 %. As can be established by the Fresnel equations and the measured angular dependence, the reflectance changes by less than 0.2 % when the angle of incidence varies from 0° to 4° . Therefore, within the uncertainty

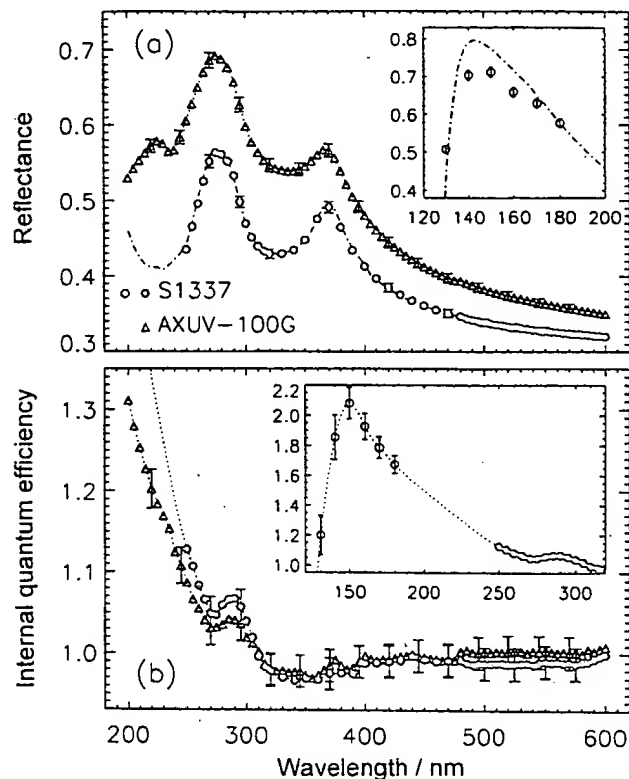


Figure 4. (a) Measured reflectance at 4° incidence angle of an S1337 Si pn photodiode and an AXUV-100G Si np photodiode in the 200 nm to 600 nm spectral range. The dot-dashed line shows the reflectance as calculated from the optical constants [16, 17] for an oxide thickness of 27 nm using the Fresnel equations.

Inset: measured reflectance at 4° incidence angle of an S1337 photodiode in the 130 nm to 180 nm wavelength range.

(b) Inferred internal quantum efficiency of the two diode types in their respective spectral ranges of stable response. Inset: initial internal quantum efficiency of an S1337 photodiode in the 130 nm to 180 nm wavelength range. Please note that the dotted lines are simply guides to the eye.

of our measurement, the curves in Figure 4a also represent the normal-incidence reflectance of the diodes.

The inset of Figure 4a shows additional data on the reflectance at 4° angle-of-incidence of an S1337 photodiode in the 130 nm to 180 nm spectral range. In this wavelength range the spectral responsivity of the S1337 is subject to rapid radiation damage, and

Table 1. Spatial nonuniformity and resulting uncertainty contribution to the spectral responsivity for the different diode types. (a) Relative standard deviation of the local responsivity in a circular area of 6 mm in diameter about the diode centre. The measurement was performed with a 257.3 nm laser beam focused to a circular spot of 0.25 mm diameter. (b) Values apply to a beam of 2 mm \times 1 mm FWHM centred to within ± 0.5 mm of the diode centre.

	Diode type			
	Si pn S1337/S5226	Si np UVG-100	Si np AXUV-100G	Schottky PtSi-n-Si
(a) 100 \times relative spatial nonuniformity	0.06	0.4	0.14	0.5
(b) 100 \times contribution to relative uncertainty of spectral responsivity	0.006	0.08	0.013	0.09

the purpose of the reflectance measurements was to investigate whether the change in spectral responsivity was accompanied by a change in reflectance. In the wavelength range investigated from 130 nm to 180 nm, however, no change in reflectance was observed. The dot-dashed line is a calculation based on the Fresnel equations using literature data for the optical constants [16, 17] and assuming a thickness of 27 nm for the silicon-oxide layer. While the calculation fits the reflectance data of the S1337 excellently in the 250 nm to 600 nm spectral range, the reflectance at shorter wavelengths is overestimated. This discrepancy is attributed to the optical constants of the silicon-oxide passivation layer being at variance with the literature data, for example due to a non-stoichiometric composition of the oxide.

Figure 4b shows the internal quantum efficiency η_{int} of the AXUV-100G and the S1337 photodiodes as derived from the measured spectral responsivity s (Figure 1) and the reflectance at normal incidence ρ via the identity

$$\eta_{\text{int}} = \frac{hc}{\lambda e} \frac{s}{1 - \rho} \quad (2)$$

The internal quantum efficiency η_{int} is a property of the photodiode, namely the number of *detected* electron-hole pairs per photon absorbed in the diode *including the front layer*. For an ideal diode with a non-absorbing front layer and no internal charge collection losses, η_{int} would be identical to the quantum yield of silicon η_{Si} , which is a material property, i.e. the number of *created* electron-hole pairs per photon absorbed in the silicon bulk.

For the S1337 and AXUV-100G photodiodes the internal losses are small, and the oxide-passivation layer is transparent in the 200 nm to 600 nm spectral range. Hence, the increase of the internal quantum efficiency towards shorter wavelengths seen in Figure 4b reflects the increase in quantum yield of silicon due to impact ionization of the photogenerated charge carriers [18, 19]. Apart from confirming the presence of the structure around 290 nm wavelength [20, 21], our data suggest that the further increase of the quantum yield of silicon previously reported for wavelengths down to 250 nm [22] continues monotonically at least down to the 200 nm wavelength without further features.

As is seen from the inset in Figure 4b, which includes the additional data on the initial internal quantum efficiency of an S1337 photodiode in the 130 nm to 180 nm spectral range, the internal quantum efficiency continues to increase with decreasing wavelength down to wavelength 150 nm. The decrease of η_{int} seen at wavelengths below 150 nm is due to the onset of absorption in the oxide-passivation layer. In this wavelength range the internal quantum efficiency of the photodiode as given by (2) ceases to reflect the spectral dependence of the quantum yield of silicon.

Our data suggest that the two diode types have about the same internal quantum efficiency in the

300 nm to 600 nm spectral range, with some indication that for wavelengths shorter than 300 nm the S1337 has a slightly higher internal quantum efficiency than does the AXUV-100G. As the S1337 photodiode was reported to have internal losses of about 2.5 % at about 400 nm with an increasing trend towards shorter wavelengths [23], even greater losses must be concluded for the AXUV-100G. Hints to the presence of significant (several percent in magnitude) recombination losses in AXUV-100G have also been found in experiments in the soft x-ray spectral range [24]. Using the same model for the charge-collection efficiency and the identical parameters as in [25], we found the internal losses of the AXUV-100G photodiode to be negligible for wavelengths above 380 nm, but to amount to about 6 % in the 120 nm to 320 nm spectral range.

In their study of np photodiodes of the AXUV-100G and UVG-100 types, Canfield et al. [26] assumed that the diodes have no internal losses. The quantum-yield values they obtain for the 160 nm to 250 nm wavelength range, which are in fact the internal quantum efficiencies of their np diodes, are about 20 % higher than our values as shown in Figure 4b. This discrepancy cannot be attributed to a different extent of radiation damage (e.g. for the S1337 in the 130 nm to 180 nm interval), as this effect has already been accounted for by the larger uncertainties. It is more likely that the disagreement is due to the fact that Canfield et al. used a calculation of the reflectance based on the Fresnel equations and literature data for the optical constants, whereas in our case the reflectance was actually measured. We found that, in the case of the S1337 photodiode, the Fresnel calculation (dot-dashed line in Figure 4a) underestimates the reflectance at 160 nm wavelength, for example, by about 10 %, which in turn leads to a relative overestimation of the internal quantum efficiency by about 15 %. For the nitrided-oxide passivation layer of the np photodiodes, the literature data for the optical constants may be even less appropriate due to the oxygen deficiency of the nitrided oxide, established in reflectance measurements on AXUV-100G diodes in the soft x-ray spectral range [27].

For the PtSi-n-Si Schottky-barrier diodes, the reflectance measurements have been carried out over the whole 120 nm to 600 nm spectral range. Figure 5a shows the measured reflectance spectrum at 4° angle-of-incidence. The results for the internal quantum efficiency are presented in Figure 5b. Due to its metallic character, the PtSi front layer is strongly absorbing over the entire spectral range of this investigation and hence the spectral shape of the internal quantum efficiency of the photodiode is no longer dominated by the material properties of silicon. A detailed report of the studies on the PtSi-n-Si photodiodes will be published elsewhere, as a discussion of all the information contained in the reflectance measurements at different angles, including the optical constants of the platinum-silicide layer, is beyond the scope of this communication.

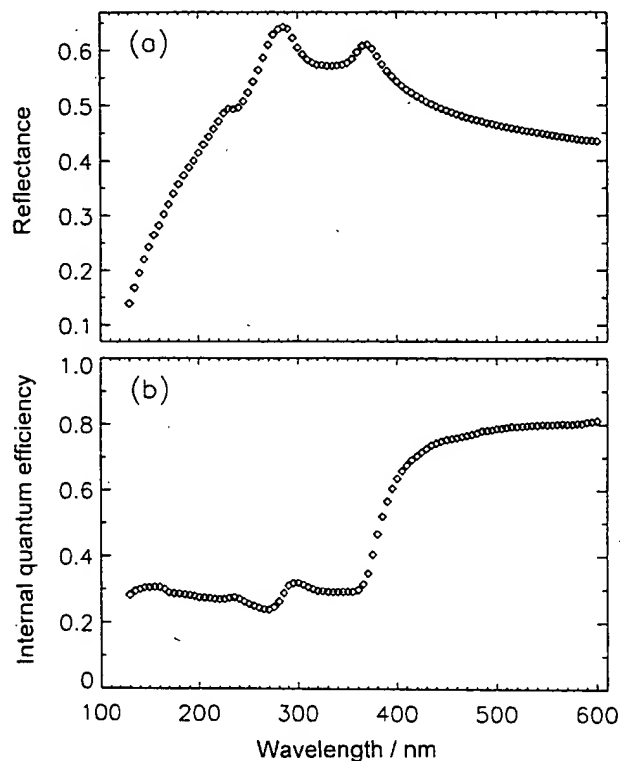


Figure 5. (a) Measured reflectance at 4° incidence angle of a PtSi-n-Si Schottky-barrier photodiode in the 120 nm to 600 nm spectral range. (b) Internal quantum efficiency of the PtSi-n-Si Schottky-barrier photodiodes.

6. Mean energy required to produce an electron-hole pair in silicon

We have used the data on the internal quantum efficiency η_{int} of the oxide-passivated diffusion-type photodiodes, as shown in Figure 4b, to derive the wavelength-dependence of the quantum yield η_{Si} of silicon. In order to do so, we used published data for the internal losses of the S1337 photodiode at wavelengths above 400 nm [23], and the model presented in [25] to describe the internal losses of the AXUV-100G photodiode in the 200 nm to 400 nm wavelength range. For the actual calculation of the losses, we included only the front-surface collection efficiency and used the values of the relevant model parameters that have been derived for AXUV-100G photodiodes from measurements in the soft x-ray spectral range [25]. The same model, but with adjusted parameters, was also used to extrapolate the internal losses of the S1337 photodiode to wavelengths below 400 nm. In the 250 nm to 400 nm wavelength range, the results for η_{Si} derived from the two diode types were considered as upper and lower boundaries, and the final result was taken to be the average of the two.

For a more convenient presentation of the results we use the mean energy required to produce an electron-hole pair ("pair-creation energy"), W_{Si} , which is related to the quantum yield η_{Si} by $W_{\text{Si}} = h\nu/\eta_{\text{Si}}$. Figure 6

shows our results for W_{Si} together with the data of [25] for the soft x-ray spectral range. To aid presentation, the wavelength axis is logarithmic for wavelengths up to 100 nm and linear above 100 nm. Filled circles represent the averaged results derived from S1337 and AXUV-100G photodiodes in the wavelength range above 250 nm; the standard relative uncertainty of these data points is about 2%. The data points marked by open circles originate from the reflectance measurements on an S1337 photodiode in the 130 nm to 180 nm spectral range and correspond to the data shown in the inset of Figure 4b. For these data points, the standard relative uncertainty of the experimentally determined W_{Si} values ranges from about 4% to about 6%. The open triangles are data points derived from AXUV-100G diodes. For the soft x-ray spectral range, at wavelengths below 25 nm, the relative uncertainty of the mean pair-creation energy is in the range 0.6% to 1.4%, depending on wavelength [25].

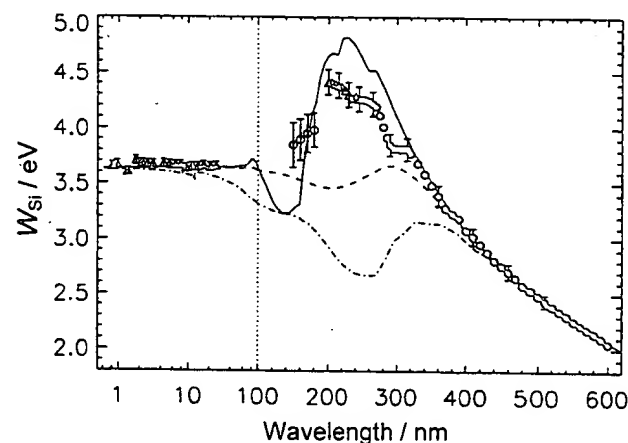


Figure 6. Spectral dependence of the mean energy W_{Si} to produce an electron-hole pair in crystalline silicon by absorption of a photon in the wavelength range 0.8 nm to 600 nm. Filled circles: averaged results derived from S1337 and AXUV-100G photodiodes at wavelengths where both diodes are stable (see text); open circles: S1337; open triangles: AXUV-100G. The data points for the 0.8 nm to 25 nm wavelength range are taken from [25].

The curves give results of theoretical calculations [25] based on different assumptions as to the amount of kinetic energy transferred to the hole upon photoabsorption in the valence band. Short-dashed line: uniform distribution of all possible hole energies; dot-dashed line: zero kinetic energy of hole (absorption only from valence-band maximum); solid line: kinetic energy of hole equal to electron kinetic energy or to valence-band width, whichever is smaller.

The vertical dotted line separates the ranges where the wavelength scale is logarithmic and where it is linear.

It should be noted that the data in the 200 nm to 250 nm spectral range derived from AXUV-100G diodes, are only regarded as an upper estimate of W_{Si} . The possible change of optical constants due to the oxygen deficiency of the nitrided-oxide of the AXUV-100G diodes would be expected to shift the absorption

edge of the oxide towards longer wavelengths. Thus the data from AXUV-100G diodes may be corrupted from absorption in the passivation layer. Taking this word of caution into account, our experimental results indicate that W_{Si} reaches a maximum in the 200 nm to 250 nm wavelength range and then tends to decrease with decreasing wavelength and approaches the constant value of the soft x-ray spectral range, $W_{Si} = 3.66$ eV [25].

The three lines in Figure 6 are the results of theoretical calculations of W_{Si} from literature data of the photoabsorption coefficient, ionization rates for the photogenerated charge carriers, and branching ratios for the decay of the core-excited atom. The calculations differ in their assumptions concerning the kinetic energy distribution of the holes after photoabsorption in the valence band. The dot-dashed line corresponds to the case where only electrons at the top of the valence band take part in the photoabsorption process. As was established in [24], this assumption is unrealistic and leads to an underestimation of W_{Si} , whereas the suppositions that the kinetic energy of the hole takes each possible value with the same probability (short-dashed line), or that it equals the kinetic energy of the electron (as long as this value is less than the width of the valence band, or takes its maximum value; solid line), make no significant difference in the soft x-ray range. In the UV and VUV spectral ranges the two assumptions yield clearly different spectral shapes for the W_{Si} value. Whereas an equal distribution of hole energies results in an almost constant W_{Si} up to wavelengths in the near-UV, the calculation based on an equal partition of energy between electron and hole gives a spectral dependence that is in reasonable qualitative agreement to the experimental data (Figure 6).

7. Conclusions

We have investigated several different types of photodiode for their suitability as transfer detector standards in the 120 nm to 600 nm spectral range. Their spectral responsivity was determined with the SYRES cryogenic radiometer with a relative uncertainty of about 0.7 % to 1 %. The spectral responsivity of all photodiodes is of the order of 0.1 A W^{-1} in the spectral range of this study. The most pronounced spectral features are found for the UVG-100 np-junction diode, due to the large oxide thickness. The UVG-100 and the PtSi-n-Si Schottky-type diodes show a significantly higher spatial nonuniformity than do the pn-junction diodes.

The spectral responsivity of the S1337 and S5226 pn-junction photodiodes shows a rapid decrease with increasing radiant exposure when irradiated at wavelengths shorter than 250 nm. For the np-junction diodes, radiation damage is also found for irradiation at certain wavelengths. The UVG-100 photodiodes exhibit

an initial degradation rate comparable with that of the pn-junction diodes at wavelengths between 175 nm and 250 nm. For the AXUV-100G photodiode, degradation is encountered for wavelengths between 125 nm and 225 nm. Only the PtSi-n-Si photodiodes showed no degradation over the spectral range of this investigation, and therefore seem to be the only candidates for the realization of a uniform spectral-responsivity scale for the whole UV spectral range.

In addition, reflectance measurements have been performed on the photodiodes to determine the internal quantum efficiency with a typical relative uncertainty of about 2 %. The internal quantum efficiencies of the S1337 Si pn-photodiode and of the AXUV-100G Si np-photodiode were found to be almost equal. Combined with measurements at shorter wavelengths and a parametrization of the front-surface losses taken from the literature, the mean pair-creation energy W_{Si} was derived. The data suggest that the W_{Si} for photoabsorption in silicon reaches a maximum in the 200 nm to 250 nm spectral range, and tends to approach the almost constant value of $W_{Si} = 3.66$ eV that was reported recently for the soft x-ray spectral range, presumably at a wavelength of about 100 nm.

References

1. Fox N. P., *Metrologia*, 1995/96, **32**, 535-544.
2. Gentile T. R., Houston J. M., Cromer C. L., *Appl. Opt.*, 1996, **35**, 4392-4403.
3. Köhler R., Goebel R., Pello R., *Metrologia*, 1995/96, **32**, 463-468.
4. White M. G., Bittar A., *Metrologia*, 1993, **30**, 361-364.
5. Fischer J., Fu L., *Appl. Opt.*, 1993, **32**, 4187-4190.
6. Fox N. P., *Metrologia*, 1991, **28**, 197-202.
7. Durant N. M., Fox N. P., *Metrologia*, 1995/96, **32**, 505-508.
8. Solt K., Melchior H., Kroth U., Kuschnerus P., Persch V., Rabus H., Richter M., Ulm G., *Appl. Phys. Lett.*, 1996, **69**, 3662-3664.
9. Korde R., Geist J., *Appl. Opt.*, 1987, **26**, 5284-5290.
10. Korde R., Cable J. S., Canfield L. R., *IEEE Trans. Nucl. Science*, 1993, **40**, 1655-1659.
11. Rzeghi M., Rogalski A., *J. Appl. Phys.*, 1996, **79**, 7433-7473.
12. Rabus H., Persch V., Ulm G., *Appl. Opt.*, 1997, **36**, 5421-5440.
13. Werner L., Ultraviolet stability of silicon photodiodes, *Metrologia*, 1998, **35**, 407-411.
14. Fu L., Fischer J., *Metrologia*, 1993, **30**, 297-303.
15. Fuchs D., Krumrey M., Lederer T., Müller P., Scholze F., Ulm G., *Rev. Sci. Instrum.*, 1995, **66**, 2248-2251.
16. Phillip H. R., In *Handbook of Optical Constants of Solids*, 1st ed. (Edited by E. D. Palik), London, Academic Press, 1985.
17. Malitson I. H., *J. Opt. Soc. Am.*, 1965, **55**, 1205-1217.
18. Geist J., Gardner J. L., Wilkinson F. J., *Phys. Rev. B*, 1990, **42**, 1262-1267.
19. Kolodinski S., Werner J. H., Wittchen T., Queisser H. J., *Appl. Phys. Lett.*, 1993, **63**, 2405-2407.
20. Wilkinson F. J., Farmer A. J. D., Geist J., *J. Appl. Phys.*, 1983, **54**, 1172-1174.

21. Bittar A., *Metrologia*, 1995/96, **32**, 497-500.
22. Durant N. M., Fox N. P., *Metrologia*, 1993, **30**, 345-350.
23. Stock M., Fischer J., Friedrich R., Jung H. J., Thornagel R., Ulm G., Wende B., *Metrologia*, 1993, **30**, 439-449.
24. Scholze F., Rabus H., Ulm G., *Appl. Phys. Lett.*, 1996, **69**, 2974-2976.
25. Scholze F., Rabus H., Ulm G., accepted by *J. Appl. Phys.*
26. Canfield L. R., Vest R. E., Korde R., Schmidtke H., Desor R., *Metrologia*, 1998, **35**, 329-334.
27. Scholze F., Rabus H., Ulm G., *Proc. SPIE*, 1996, **2808**, 534-543.